ISBN: 978-3-95450-240-0 ISSN: 2673-5539 doi:10.18429/JACoW-RuPAC2021-MOPSA41

EFFECT OF A PROTON BEAM FROM A LINEAR ACCELERATOR FOR RADIATION THERAPY

L. Ovchinnikova*[1], S. Akulinichev, A. Durkin, A. Kolomiets, V. Paramonov
INR RAS, Moscow, Russia
A. Kurilik, Moscow, Russia
[1]also at Ferrite Domen Co., St. Petersburg, Russia

Abstract

Linear accelerators can provide beam characteristics that cannot be achieved by circular accelerators. We refer to the concept of a compact linac for creating a proton accelerator with a maximum energy of 230 MeV, operating in a pulsed mode. The linac is designed to accelerate up to 10^{13} particles per 10 to 200 seconds irradiation cycle and is capable of fast adjustment the output energy in the range from 60 to 230 MeV, forming a pencil-like beam with a diameter of ~2 mm. Simulation of dose distribution from a proton beam in a water phantom has been performed. The radiological effect of the linac beam during fast energy scanning is considered, and the features for providing the high dose rate FLASH radiation therapy are specified. The possibility of a magnetic system for increasing the transverse dimensions of the beam-affected region is discussed.

INTRODUCTION

Cancer

Cancer is the second leading cause of death worldwide, as noted by the World Health Organization [1]. The probability of cancer in general population is dependent on genetic predisposition, gender, age, environmental factors, lifestyle and past illnesses [2, 3]. Various preventive strategies, early diagnosis, efficiency and accessibility of applicable types of treatment contribute to the odds of a favorable outcome.

Proton Therapy

Radiation therapy is one one of the most widely used non-surgical methods of malignant tumor treatment. External beam radiation therapy is the method of choice when dealing with deep pathological foci. Gamma rays from various radiation sources, bremsstrahlung photons and electrons produced by electron accelerators, and protons, neutrons and ions originating from hadron accelerators provide the required penetration into body tissue. Proton beams allow to achieve good localization of therapeutic dose delivery while minimizing collateral damage to healthy tissue [4].

Linac Advantages

Linear accelerators provide numerous advantages over circular accelerators. Combination with gantry is possible [5]. This type of accelerator enables precise beam energy modulation while eliminating the necessity for auxiliary energy changes. It also eliminates the losses, parasitic material activation and elevated background radiation levels associated with beam extraction from circular orbits. In this work, we focus on the linear proton accelerator concept, as described in [6].

DOSE DELIVERY

There are several methods of dose distribution forming in patient's body, used throughout the long-standing history of proton therapy, passive scattering being the most traditional one, and involving the use of collimation and compensation equipment. This method causes excessive patient irradiation by nuclear reaction products and necessitates safe storage of single-use collimators and compensators before disposing or recycling.

Beam scanning method eradicates these inconveniences and allows to apply almost arbitrary dose distribution [7, 8]. Also, proton arc therapy is promising [9, 10].

BEAM MANIPULATION

Most of the units put in operation over the past five years in the USA make use of gantries and Pencil Beam Scanning [11]. In this work, we focus on Pencil Beam Scanning with energy up to 250 MeV. Consequently, beam transportation and dose distribution forming are the most important research objectives.

Non-linear magnetic systems are often used to achieve uniform lateral dose distribution. A single non-linear magnet can be used for uniform dose distribution in a single plane [12]. Such magnets are designed for specific mean-square beam radius, [13] describing an auxiliary mechanical device for additional field tuning. Such device allows a beam be stretched into a line in a single plane, e.g. horizontal. This way, scanning can be used in a vertical plane, facilitating strip scanning, similarly minibeam [14, 15].

We also consider the use of dual scanning magnets in vertical and horizontal planes [16], this type of installation providing the most simple and versatile irradiation method. We also take into account that additional simulation is necessary when choosing the best method to achieve the desired distribution when dealing with distant tumor patches. A magnetic multipole combination [17–20] should be used when uniform distribution is desired. Such combination allows for wide beam energy range, facilitating beam width modulation. One can also use permanent magnets when designing achromatic turn only beam transportation system [21].

* lub.ovch@yandex.ru

ISBN: 978-3-95450-240-0 ISSN: 2673-5539 doi:10.18429/JACoW-RuPAC2021-MOPSA41

GEANT4 SIMULATION PROCEDURE

PSTAR [22] data was used for preliminary projected proton range estimation depending on the kinetic energy. The ~158 mm range corresponds to the mean energy of 150 MeV. Geant4 was used to simulate proton dose distributions in a volume [23]. Beam dynamics simulation results described in [6] were used to estimate the accelerator beam parameters and the resulting dose field parameters. TRANSIT [24] output files have been converted to input for Geant4. Particles at the accelerator nozzle were used. Beam radius used in simulation was $r_{RMS} < 0.35$ mm, with energy deviation $e_{RMS} < 0.057$ %. As for our task, dose calculation can be performed with accelerator beam approximated as an monoenergetic pencil beam.

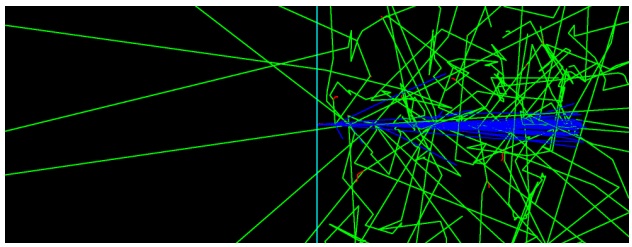

Figure 1: Trajectories visualization in Geant4. Neutral particle tracks shown in green, positively charged particle tracks shown in blue, negatively charged particle tracks shown in red, cyan line marks water phantom boundary.

It was assumed that the simulated particle beam immediately enters the half-space filled with water (Fig. 1). The absorbed dose accumulation is performed in 1 mm steps in the area of ± 50 mm on X and Y axes, 0 to 400 mm on Z axis. X axis is pointing to the right, Y axis is pointing up, Z axis coincides with beam vector.

SIMULATION RESULTS

Depth Dose Distribution

A uniform depth dependency was initially used with the aim of assessing the capability of the described accelerator [6] to form the uniform dose distribution. A spread out Bragg peak with absorber-modulated energy is usually used is such cases. In our case, energy is modulated by the accelerator itself. The sum of the Bragg curves and the corresponding scale factors k are shown in the Fig. 2. The dose characteristics are shown in the Table 1.

Table 1: Characteristics of Absorbed dose distribution by depth

Characteristic	Value
Accumulated pulse duration (μs)	48.2
Protons per 1 μs	10^{10}
Average dose (Gy)	6.52
Dose standard deviation (%)	2.24
Dose Uniformity Ratio = Dmax / Dmin	1.11

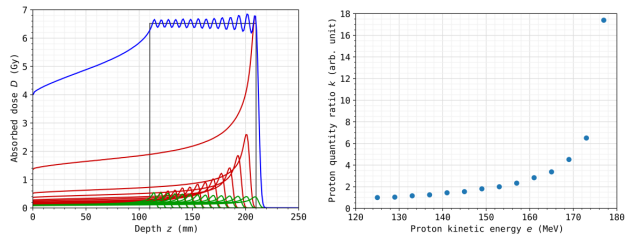

(a) (b)

Figure 2: Uniform dose distribution by depth, consisting of several Bragg curves — (a). The curves are obtained by averaging the volumetric dose in a volume with 100 × 100 mm transverse dimensions. Irradiation volume limited by 110 to 220 mm depth along Z axis is shown in grey color. Bragg curves of 122 up to 177 MeV protons with 4 MeV increment are shown in green color. There are 14 energies in total. The number of protons is 10^{10} for each energy. Bragg curves multiplied by scale factors are shown in red. Accumulated dose is shown in blue. Scale factors — (b).

For the lowest energy of 125 MeV the scale factor $k = 1$, which corresponds to the number of protons 10^{10}. The highest energy 177 MeV corresponds to $k = 17.4$, or $17.4 \cdot 10^{10}$ protons. That means that the higher the energy, the more protons are needed to achieve the desired dose. The sum of scale factors is 48.2, or $48.2 \cdot 10^{10}$ protons in total. Therefore, the total dose in a volume of $100 \times 100 \times 100$ mm^3 is 6.52 Gy when using passive beam scattering, and that dose is delivered over 48.2 microseconds of accumulated accelerator pulse duration.

3D Dose Distribution

We have simulated the filling of $100 \times 100 \times 100$ mm^3 volume using Pencil beams with spot step 4 mm and Gaussian distributed beams with $\sigma = 11$ mm and spot step 25 mm in transverse plane. The inhomogeneity of the spatial distribution of the absorbed dose should be small [25].

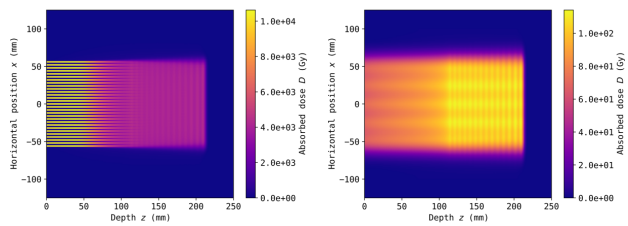

Figure 3: The dose distribution in ZX plane intersecting in dose peaks. Left — Pencil beams, right — Gaussian distributed beams with $\sigma = 11$ mm.

The Fig. 3–8 and Table 2 show the calculation results. Our calculations point out that pencil beams deliver very high average dose, which is orders of magnitude higher than the required therapeutic dose. With wide gaussian beams the average dose can be lowered to FLASH mode levels when using wide beams. FLASH mode requires shortening of irradiation time to 0.5 seconds [26]. Thus, the particle

ISBN: 978-3-95450-240-0 ISSN: 2673-5539 doi:10.18429/JACoW-RuPAC2021-MOPSA41

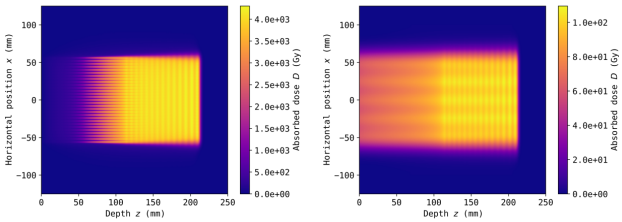

Figure 4: The dose distribution in ZX plane intersecting in dose valley. Left — Pencil beams, right — Gaussian distributed beams with σ = 11 mm.

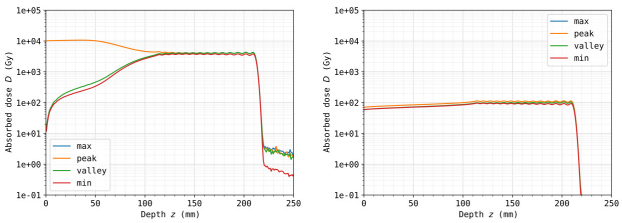

Figure 5: Dose distributions as functions of depth in dose peak and dose valley. Left — Pencil beams, right — Gaussian distributed beams with σ = 11 mm.

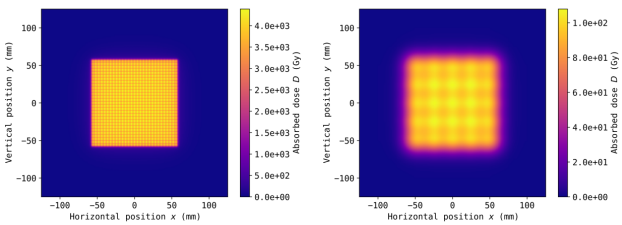

Figure 6: XY plane dose distribution for 110 mm depth. Left — Pencil beams, right — Gaussian distributed beams with σ = 11 mm.

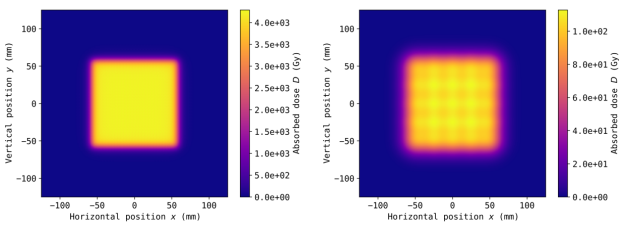

Figure 7: XY plane dose distribution for 210 mm depth. Left — Pencil beams, right — Gaussian distributed beams with σ = 11 mm.

accelerator under consideration can provide FLASH mode irradiation to a volume less than 100 × 100 × 100 mm^3.

CONCLUSIONS

- In order to meet FLASH mode requirements when using beam scanning technique, the accelerator beam can be widened and flattened using nonlinear magnetic elements.
- Alternatively, pulse charge can be lowered and pulse frequency increased accordingly.

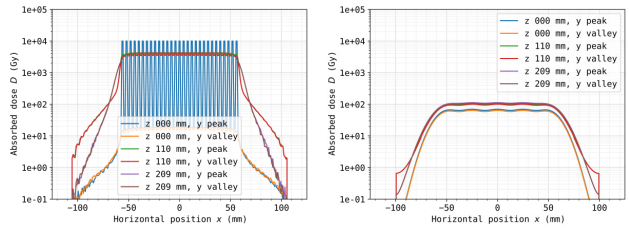

Figure 8: Dose as a function of x along peak and valley for different depth values. Left — Pencil beams, right — Gaussian distributed beams with σ = 11 mm.

Table 2: Absorbed dose distribution characteristics in 100 × 100 × 100 mm^3 volume

Characteristic	Pencil beams	Gaussian beams
Spot step (mm)	4	25
Spots num	841	25
Accumulated pulse duration (μs)	40536	1205
Average dose (Gy)	4006	102
Minimal dose (Gy)	3300	83.4
Maximal dose (Gy)	4481	114
Dose standard deviation (%)	3.36	4.27
Dose Uniformity Ratio = Dmax / Dmin	1.36	1.37

- It should be taken into account that FLASH therapy has some time–dependent limitations [27, 28].
- It is necessary to simulate the beam spread in the vacuum window and in the air between nozzle and water phantom [29, 30].

ACKNOWLEDGEMENTS

The authors thanks colleagues in INR RAS for fruitful discussions and valuable comments. Especially thanks to L. Kravchuk and A. Feschenko for their support of the work, useful discussions and recommendations.

REFERENCES

[1] World Health Organization, *WHO report on cancer: setting priorities, investing wisely and providing care for all*. World Health Organization, 2020, 149 p. ISBN: 978-92-4-000129-9.

[2] American Cancer Society, *Global Cancer Facts & Figures 4th Edition*. Atlanta: American Cancer Society, 2018.

[3] American Cancer Society, *Cancer Treatment & Survivorship Facts & Figures 2019–2021*. Atlanta: American Cancer Society, 2019.

[4] H. Paganetti, *Proton Beam Therapy*, ser. 2399-2891. IOP Publishing, 2017. DOI: 10.1088/978-0-7503-1370-4.

[5] C. Cuccagna *et al.*, "Beam parameters optimization and characterization for a TUrning LInac for Protontherapy," *Physica Medica*, vol. 54, pp. 152–165, 2018. DOI: 10.1016/j.ejmp.2018.08.019.

ISBN: 978-3-95450-240-0 ISSN: 2673-5539 doi:10.18429/JACoW-RuPAC2021-MOPSA41

[6] V. Paramonov, A. Durkin, and A. Kolomiets, "A Linear Accelerator for Proton Therapy", presented at RuPAC'21, September 2021, paper FRB04, this conference.

[7] T. Haberer, W. Becher, D. Schardt, and G. Kraft, "Magnetic scanning system for heavy ion therapy," *Nuclear Instruments and Methods in Physics Research Section A: Accelerators, Spectrometers, Detectors and Associated Equipment*, vol. 330, no. 1, pp. 296–305, 1993. DOI: 10.1016/0168-9002(93)91335-K.

[8] E. Pedroni *et al.*, "The 200-MeV proton therapy project at the Paul Scherrer Institute: Conceptual design and practical realization," *Medical Physics*, vol. 22, no. 1, pp. 37–53, 1995. DOI: 10.1118/1.597522.

[9] S. Ferguson, S. Ahmad, and I. Ali, "Simulation study of proton arc therapy with the compact single-room MEVION-S250 proton therapy system," *Journal of Radiotherapy in Practice*, vol. 19, no. 4, pp. 347–354, 2020. DOI: 10.1017/S1460396919000888.

[10] X. Ding, X. Li, J. M. Zhang, P. Kabolizadeh, C. Stevens, and D. Yan, "Spot-Scanning Proton Arc (SPArc) Therapy: The First Robust and Delivery-Efficient Spot-Scanning Proton Arc Therapy," *International Journal of Radiation Oncology*Biology*Physics*, vol. 96, no. 5, pp. 1107–1116, 2016. DOI: 10.1016/j.ijrobp.2016.08.049.

[11] Particle Therapy Co-Operative Group, *Particle therapy facilities in clinical operation*. https://www.ptcog.ch/index.php/facilities-in-operation

[12] A. J. Jason, B. Blind, and K. Halbach, "Beam expansion with specified final distributions," in *PAC'97 Proceedings*, 1998, pp. 3728–3730. https://accelconf.web.cern.ch/pac97/papers/pdf/9P052.PDF

[13] G. Gu and W. Liu, "Uniformization of the Transverse Beam Profile by a New Type Nonlinear Magnet," in *Proc. 6th International Particle Accelerator Conference (IPAC'15), Richmond, VA, USA, May 3-8, 2015*, (Richmond, VA, USA), ser. International Particle Accelerator Conference, Geneva, Switzerland: JACoW, Jun. 2015, pp. 272–274. DOI: 10.18429/JACoW-IPAC2015-MOPWA065.

[14] J. Reindl and S. Girst, "pMB FLASH - Status and Perspectives of Combining Proton Minibeam with FLASH Radiotherapy," *Journal of Cancer Immunology*, vol. 1, pp. 14–23, Aug. 2019. DOI: 10.33696/cancerimmunol.1.003.

[15] A. Mazal *et al.*, "FLASH and minibeams in radiation therapy: The effect of microstructures on time and space and their potential application to protontherapy," *The British Journal of Radiology*, vol. 93, no. 1107, p. 20 190 807, 2020. DOI: 10.1259/bjr.20190807.

[16] J. Kolski, "Proposed Varying Amplitude Raster Pattern to Uniformly Cover Target for the Isotope Production Facility (IPF) at LANSCE," in *Proceedings of HB2014*, 2014, pp. 148–150. https://accelconf.web.cern.ch/HB2014/papers/mopab46.pdf

[17] N. Tsoupas *et al.*, "Uniform beam distributions at the target of the NASA Space Radiation Laboratory's beam line," *Phys. Rev. ST Accel. Beams*, vol. 10, p. 024 701, 2 Feb. 2007. DOI: 10.1103/PhysRevSTAB.10.024701.

[18] Y. Yuri, N. Miyawaki, T. Kamiya, W. Yokota, K. Arakawa, and M. Fukuda, "Uniformization of the transverse beam profile by means of nonlinear focusing method," *Phys. Rev. ST Accel. Beams*, vol. 10, p. 104 001, 10 Oct. 2007. DOI: 10.1103/PhysRevSTAB.10.104001.

[19] Y. Yuri, I. Ishibori, T. Ishizaka, S. Okumura, and T. Yuyama, "Uniform Beam Distribution by Nonlinear Focusing Forces," in *Proceedings of IPAC'10*, 2010, pp. 4149–4151. https://accelconf.web.cern.ch/IPAC10/papers/thpec041.pdf

[20] I. Ivanenko, I. Kalagin, V. Kazacha, and N. Kazarinov, "Getting Uniform Ion Density on Target in High-Energy Beam Line of Cyclotron U-400M with Two," in *Proceedings of Cyclotrons2013*, 2013, pp. 335–337. https://accelconf.web.cern.ch/CYCLOTRONS2013/papers/weppt007.pdf

[21] D. Trbojevic, S. Brooks, T. Roser, and N. Tsoupas, "Superb Fixed Field Permanent Magnet Proton Therapy Gantry," in *Proc. IPAC'21*, (Campinas, SP, Brazil), ser. International Particle Accelerator Conference, JACoW Publishing, Geneva, Switzerland, Aug. 2021, TUPAB030, pp. 1405–1408. DOI: 10.18429/JACoW-IPAC2021-TUPAB030.

[22] NIST Physical Measurement Laboratory. "Stopping-power & range tables for electrons, protons, and helium ions." (2017), https://www.nist.gov/pml/stopping-power-range-tables-electrons-protons-and-helium-ions

[23] J. Allison *et al.*, "Recent developments in Geant4," *Nuclear Instruments and Methods in Physics Research Section A: Accelerators, Spectrometers, Detectors and Associated Equipment*, vol. 835, pp. 186–225, 2016. DOI: 10.1016/j.nima.2016.06.125.

[24] A. Kolomiets, A. Plastun, and T. Tretyakova, "TRANSIT code for beam dynamic simulation," in *Proceedings of RuPAC2014, Obninsk, Kaluga Region, Russia*, Oct. 2014, pp. 51–53. https://accelconf.web.cern.ch/rupac2014/papers/tupsa07.pdf

[25] H. Shu *et al.*, "Scanned Proton Beam Performance and Calibration of the Shanghai Advanced Proton Therapy Facility," *MethodsX*, vol. 6, pp. 1933–1943, 2019. DOI: 10.1016/j.mex.2019.08.001.

[26] S. Akulinichev *et al.*, "Possibilities of Proton FLASH Therapy on the Accelerator at the Russian Academy of Sciences' Institute for Nuclear Research," *Bulletin of the Russian Academy of Sciences: Physics*, vol. 84, pp. 1325–1329, Nov. 2020. DOI: 10.3103/S1062873820110039.

[27] W. Zou *et al.*, "Current delivery limitations of proton PBS for FLASH," *Radiotherapy and Oncology*, vol. 155, pp. 212–218, Feb. 2021. DOI: 10.1016/j.radonc.2020.11.002.

[28] M. Kang, S. Wei, J. I. Choi, C. B. Simone, and H. Lin, "Quantitative Assessment of 3D Dose Rate for Proton Pencil Beam Scanning FLASH Radiotherapy and Its Application for Lung Hypofractionation Treatment Planning," *Cancers*, vol. 13, no. 14, 2021. DOI: 10.3390/cancers13143549.

[29] U. Weber and G. Kraft, "Comparison of Carbon Ions Versus Protons," *Cancer journal*, vol. 15, pp. 325–32, Jul. 2009. DOI: 10.1097/PPO.0b013e3181b01935.

[30] D. Schardt, T. Elsässer, and D. Schulz-Ertner, "Heavy-ion tumor therapy: Physical and radiobiological benefits," *Rev. Mod. Phys.*, vol. 82, pp. 383–425, 1 Feb. 2010. DOI: 10.1103/RevModPhys.82.383.